Volatile Organic Compound Detection Using Insect Odorant-Receptor Functionalised Field-Effect Transistors

by

Eddyn Oswald Perkins Treacher

A thesis submitted in fulfilment of the
requirements of the degree of
Doctor of Philosophy in Physics
School of Physical and Chemical Sciences
Te Herenga Waka - Victoria University of Wellington

Oct 2023

VICTORIA UNIVERSITY OF
WELLINGTON
TE HERENGA WAKA

Acknowledgements

69450

Rifat, Alex - vapour sensor Erica Cassie - FET sensing setup Rob Keyzers and Jennie Ramirez-Garcia - NMR spectra Patricia Hunt - Computational chemistry

1. Verifying Non-Covalent Functionalisation of Carbon Nanotubes and Graphene

252732

In previous chapters, we have discussed methods of fabricating carbon nanotube and graphene devices and then shown that they can be operated effectively as chemical sensors. However, to detect specific chemical traces while ignoring others ('specific sensing'), the devices require chemical modification, often called 'functionalisation'. Instead of responding to stimuli themselves, the sensing signal is picked up by attached receptors. The devices then act as passive transducers for the received signal. Receptors previously used with carbon nanotube and graphene devices include aptamers and a range of proteins, including odorant receptors. A common approach to attaching receptors to the transducer involves the use of a linker molecule to tether the receptor to the transducer. Verifying that this linker molecule is bridging between the transducer and the receptor element is important for a complete understanding of the behaviour of these sensors. This verification involves providing evidence for effective attachment of linker molecule to the transducing device channel, then showing successful tethering of odorant receptors and other biomolecules to the attached linker molecule.

This chapter therefore takes some time to explore the attachment of linker molecules to carbon nanotube and graphene device channels, using methods such as Raman spectroscopy, fluorescence microscopy and electrical characterisation. Linker molecules used are discussed in detail, and numerous hurdles to successful functionalisation via linker molecules are identified and addressed.

1.1. Non-Covalent Functionalisation & Linker Molecules

Linker molecules may be attached via covalent or non-covalent bonding to carbon nanomaterials, such as carbon nanotubes and graphene. Non-covalent bonding is weaker and therefore less stable than covalent bonding. However, non-covalent bonding has the advantage of having less of an impact on the structure of a nanomaterial than covalent bonding, and therefore is less likely to negatively affect the electrical properties of the transducer [1]–[4]. For example, one group found covalent bonding of diazonium linker

caused a $\sim 50\%$ drop in graphene channel mobility [5]. In comparison, only a $\sim 5\%$ drop in mobility was seen for attachment of a mixture of linkers containing pyrene to a graphene channel via non-covalent π stacking [6].

π stacking or $\pi - \pi$ interaction is often used to describe a type of non-covalent bonding which occurs due to dispersion forces between unsaturated polycyclic molecules [7]. It has been argued that this label is unhelpfully specific and a misrepresentation of what can be simply classed as a type of Van Der Waals bonding [7], [8]. However, as the use of the term is widespread in the literature, it is also used here for ease of reference. Carbon nanotubes and graphene consist of a network of carbon atoms attached to each other by sp^2 hybrid orbitals in a polycyclic structure. They are therefore able to strongly interact with linker molecules with aromatic moieties, such as pyrene [4], [7], [9]. Figure 1.1 is a visual demonstration of the relationship between the pyrene-based linker molecule with the transducer and receptor elements. $\pi - \pi$ stacking with pyrene is the bonding mechanism underlying all the functionalisation processes in this thesis.
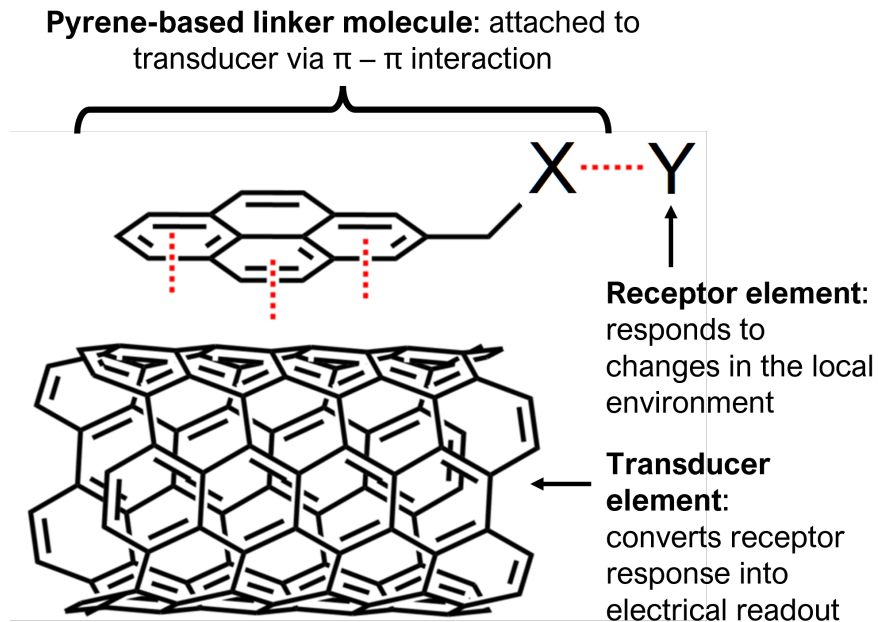

Figure 1.1.: Attachment of pyrene-based linker molecule pyrene-X and receptor Y to a carbon nanotube, representing the transducer element of a field-effect transistor. Source: Adapted from [10].

Table 1.1.: Comparison of PBASE functionalisation processes used for immobilisation of proteins and aptamers onto carbon nanotubes and graphene. Experimentally optimised variables are marked with a star (*). Blank entries indicate there was no mention of the parameter in a particular paper.

Solvent	Channel	Conc. (mM)	Incubation type	Time (hr)	Rinse steps	References
DMF	CNT	5	Immersed	1	PBS	Maehashi *et al.* [11]
		6	Immersed	1	DMF, PBS	García-Aljaro *et al.* [12]
		6	Immersed	1	DMF	Chen *et al.* [13]
		6	Immersed	1	DMF	Cella *et al.* [14]
		6	Immersed	1	DMF	Das *et al.* [15]
		6	-	2	DMF	Besteman *et al.* [16]
	Graphene	-	-	2	DMF	Kwong Hong Tsang *et al.* [17]
		-	-	20	-	Wiedman *et al.* [18]
		0.2	Immersed	20	DMF, IPA, DI water	Gao *et al.* [19]
		1	100 μL droplet	6	DMF, IPA, DI water	Nekrasov *et al.* [20]
		5	Immersed	1	DMF, DI water	Hwang *et al.* [21]
		5*	Immersed	3*	DMF	Hao *et al.* [22]
		5	Immersed, with agitation	4*	DMF, DI water	Mishyn *et al.* [4]
		6	6 μL droplet	2	DMF, DI water	Nur Nasufiya *et al.* [23]
		10	10 μL droplet	2	DMF, DI water	Campos *et al.* [24]
		10	Immersed	2	DMF, PBS	Kuscu *et al.* [25]
		10	Immersed	1	DMF	Xu *et al.* [26]
		10	Immersed	12	DMF, ethanol, DI water	Khan *et al.* [27]
		50	Immersed	4*	Methanol	Wang *et al.* [3]
2-Methoxyethanol	Graphene	1	Immersed	1	DI water	Ono *et al.* [28]
Methanol	CNT	1	Immersed	1	Methanol, DI water	Zheng *et al.* [29]
		1	Immersed	2	Methanol	Kim *et al.* [30]
		100	2 μL droplet	1	DI water	Yoo *et al.* [31]
	Graphene	5	Immersed	2	-	Sethi *et al.* [32]
		5	Immersed	1	Methanol, PBS	Ohno *et al.* [33]
DMSO	CNT	10	-	1	DI water	Lopez *et al.* [34]
		10	Immersed	1	PBS	Strack *et al.* [35]

1.1.1. 1-Pyrenebutanoic acid N-hydroxysuccinimide ester (PBASE)

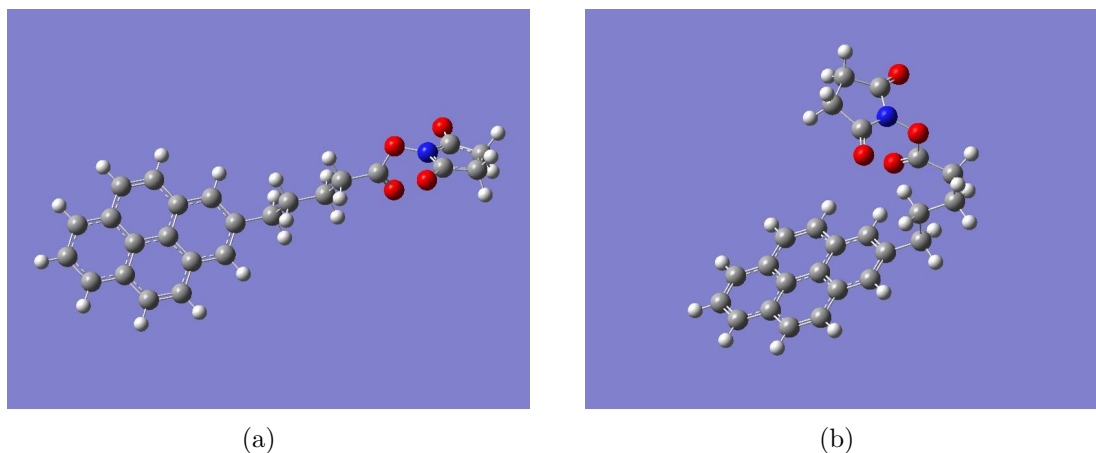<div align="center">(a)   (b)</div>

Figure 1.2.: Two conformations of PBASE molecule with geometry optimised via *ab initio* calculations (computed using Gaussian 16 [36]). White balls correspond to hydrogen, grey to carbon, red to oxygen and blue to nitrogen. The conformation in (a) has a Hartree-Fock energy of -3427728.67 kJ/mol, while the conformation in (b) has a Hartree-Fock energy of -3427729.66 kJ/mol. The difference between computed Hartree-Fock energies is 1.0 kJ/mol, small enough that the existence of both molecular conformations is physically feasible.

1-Pyrenebutanoic acid N-hydroxysuccinimide ester (variously known commercially and in the literature as 1-Pyrenebutyric acid N-hydroxysuccinimide ester, PBASE, PBSE, PASE, Pyr-NHS, PyBASE, PANHS) is a aromatic, bifunctional molecule commonly used for tethering biomolecules to the carbon rings of graphene and carbon nanotubes. The molecular structure of PBASE is shown in Figure 1.2. Two locally stable molecular conformations were found to exist, a straight (Figure 1.2a) and bent (Figure 1.2b) structure. Similar locally stable structures have previously been computed for PBASE attached to graphene [37]. The pyrene moiety, seen at the bottom of the molecular structure, non-covalently bonds to the carbon rings of the carbon nanotube and graphene surface. An N-hydroxysuccinimide (NHS) ester group is found at the top of the molecular structure, attached to the rest of the molecule via a O-C bond. The NHS ester group is highly reactive with amine groups; it can undergo a nucleophilic substitution reaction with amines attached to proteins or aptamers, tethering these biomolecules via an amide or imide bond [4], [9], [13], [38].

The non-covalent functionalisation of proteins onto a single-walled carbon nanotube using PBASE was first reported by Chen *et al.* in 2001 [13]. Two methods for protein functionalisation and immobilisation were successfully used, with the only differences being the solvent used to dissolve the PBASE powder (DMF, methanol) and the final concentration of the resulting solutions (6 mM, 1 mM respectively). The lower con-

centration may have been used for PBASE in methanol as PBASE powder appears to dissolve poorly in methanol at higher concentrations. Several groups directly cite Chen *et al.* when discussing functionalisation with PBASE [14], [16], [24], [29], [33]. Other groups using PBASE for graphene or carbon nanotube functionalisation do not explicitly reference Chen *et al.* in their methodology, but it is apparent they often draw on one of these two original methods. This common ancestry becomes apparent from the high frequency of methods detailing the use of 6 mM PBASE in dimethylformamide (DMF) and 1 mM PBASE in methanol, as seen in Table 1.1.

However, it is also apparent from Table 1.1 that there is a large degree of variation in the methods used for PBASE functionalisation. Various electrical characterisation, microscopy and spectroscopy techniques have been used to demonstrate successful functionalisation. Until recently, there has been little justification provided for the selection of variables used in the functionalisation procedure (e.g. length of time submerged in solvent containing PBASE), despite the wide-ranging use of this process in the literature [3], [39], [40]. This is surprising, given that the sensitivity of functionalised devices is considered to be closely related to the density of surface functionalisation [38], [41], [42]. Furthermore, a detailed investigation of PBASE functionalisation process variables has only been undertaken for graphene-based devices [3], [4], [22], [40].

Zhen *et al.*, Wang *et al.* and Mishyn *et al.* claim that carefully tuning the surface concentration of PBASE is required to avoid multilayer coverage of the graphene surface, as this negatively impacts sensing. Mishyn *et al.* use cyclic voltammetry to demonstrate that less receptor attachment to the graphene surface occurs when multiple layers of PBASE are present. However, neither group lends further support to their claim by performing analyte sensing using their functionalised graphene devices [4], [40]. In contrast, Hao *et al.* find that maximising surface coverage of PBASE results in more sensitive aptameric sensing, thus drawing the opposite conclusion [22]. The inconsistency in these recent findings mean more work is needed to understand the PBASE functionalisation process to achieve optimal biosensor sensitivity. It may also be the case that a specific functionalisation process is required for optimal sensitivity with the use of a specific type of receptor.

Once fastened to a bioreceptor via an amide or imide bond, the attachment to the linker molecule is not easily broken. However, prior to use in functionalisation processes, the NHS ester may react with any water present (hydrolysis). This reaction converts PBASE to 1-pyrenebutyric acid (PBA), leaving it unavailable to react further with amine groups [4], [38], [43]. If the amine group functionalisation is performed within a $ $1 hour period, with a high concentration of bioreceptor used at close to neutral pH, competing hydrolysis should not have a significantly adverse impact on the functionalisation process [38]. However, if PBASE is exposed to water during storage over a significant length of time, the presence of 1-Ethyl-3-(3-dimethylaminopropyl)carbodiimide (EDC) can be used to restore the NHS ester and enable the substitution reaction to take place (see discussion of PBA/EDC in Section 1.1.2).
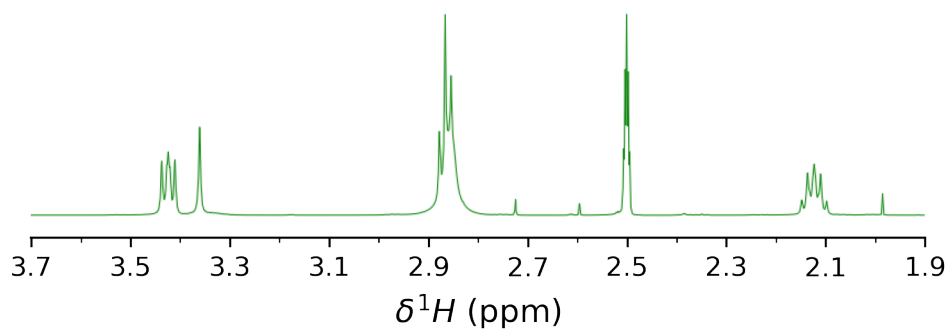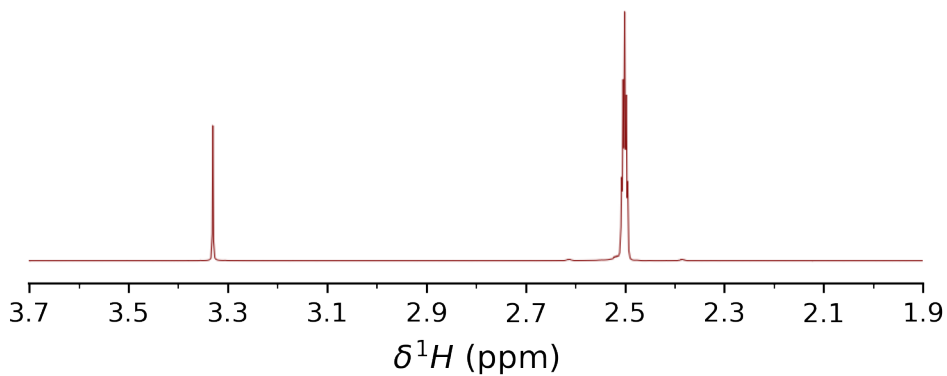
(a)
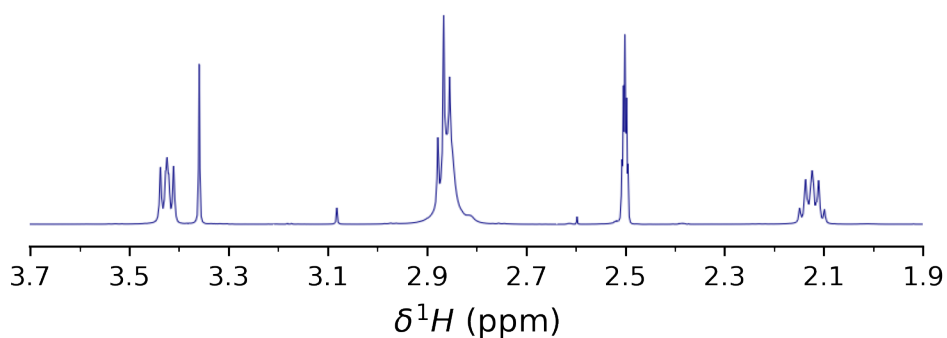
(b)

(c)

Figure 1.3.: ^{1}H Nuclear Magnetic Resonance (NMR) spectra, performed with DMSO-d$_6$ used as the NMR solvent. (a) and (b) show NMR spectrum for commercially purchased PBASE, from Sigma-Aldrich and Setareh Biotech respectively, while (c) shows the blank spectrum taken with only DMSO-d$_6$ present (spectra taken by Jennie Ramirez-Garcia).

We purchased PBASE from two suppliers, Sigma-Aldrich and Setareh Biotech. Sigma recommended DMF and methanol as suitable solvents for dissolving PBASE, alongside chloroform and dimethyl sulfoxide (DMSO). Setareh Biotech indicated methanol can be used for dissolving PBASE. The two suppliers had conflicting information for suitable storage of PBASE, with Sigma recommending room temperature storage while Setareh Biotech recommends storage of -5 to $-30°$C and protection from light and moisture. Given the long travel time of the PBASE samples under uncertain storage conditions, we used nuclear magnetic resonance (NMR) spectroscopy to verify the purity of the PBASE as recieved from each supplier. In light of the negative effect of water on PBASE, in particular we wanted to find out if any water was present in the samples.

Figure 1.3 compares the shapes of hydrogen (NMR) spectra of PBASE from each supplier when dissolved in deuterated DMSO, alongside a blank deuterated DMSO spectrum. We see both PBASE samples possess characteristic chemical shift features between $2.1 - 2.2$ ppm, $2.8 - 2.9$ ppm, and $3.4 - 3.5$ ppm. These chemical shifts roughly correspond to those seen in previous NMR spectra for PBASE [44]. The feature at 2.50 ppm represents the deuterated DMSO solvent, while the single peak between $3.3 - 3.4$ ppm represents the water present in the sample. By comparing the area of these peaks, we can estimate the amount of water originally present in the PBASE sample. The H_2O:DMSO ratio is 1:7 in the blank spectrum, but $\sim$ 1:3 in the provided samples, possibly indicating the introduction of water to the PBASE during production or storage. However, DMSO is strongly hygroscopic and slight differences in DMSO storage time, as well as differences in humidity during sample preparation, may have had a significant impact on this result [45]. Other impurities are also seen on both PBASE spectra, though their small size indicates they make up only a small percentage of each sample. Note that Strack *et al.* recommend leaving frozen PBASE at room temperature for 15 minutes before opening to prevent the introduction of condensation [35].

The electrical characteristics of the carbon nanotube or graphene transistor are often used to verify successful functionalisation and make a statement about the effect of chemical modification on the channel. However, this verification usually does not account for the effect of the solvent on the transistor channel. Figure 1.4a and Figure 1.4b show that by exposing a carbon nanotube network channel to solvents commonly used in PBASE functionalisation processes (Table 1.1), such as methanol (MeOH) or dimethyl sulfoxide (DMSO), a significant negative shift in channel threshold voltage occurs even after thorough rinsing with deionised water. Besteman *et al.* reported observing a similar effect from prolonged exposure of a single carbon nanotube to dimethylformamide (DMF) [16]. It appears that the carbon nanotubes have adsorbed solvent which persists even after device cleaning. From the shape of the change in the transfer curve, it seems the residual polar solvent molecules capacitively gate the channel [46], [47].

In contrast, previous work has shown that π-stacking carbon nanotube network to PBASE does not significantly affect the channel gating and therefore the channel threshold voltage [16], [48]. Murugathas *et al.* observed a slight increase in channel conductance after PBASE functionalisation. In Figure 1.4, we also observe a slight increase in
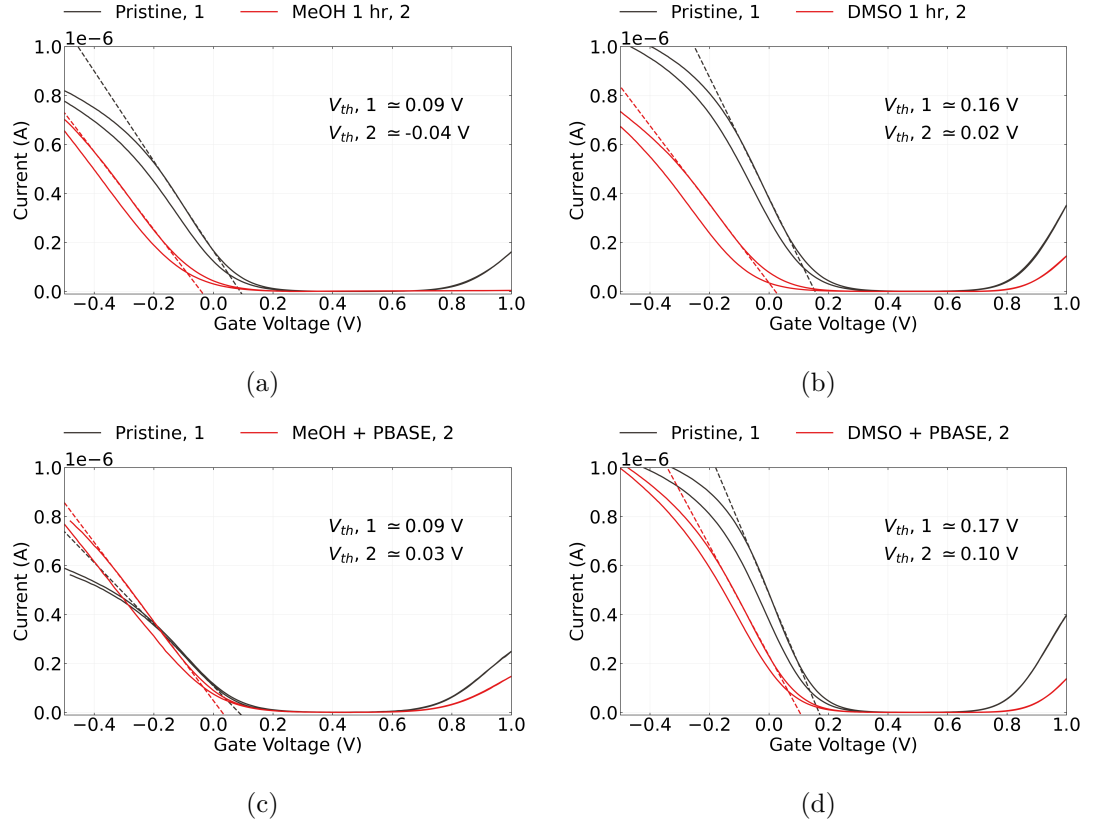
Figure 1.4.: The change in the electrical transfer characteristics of carbon nanotube transistors after being submerged in solvent for one hour and then rinsed thoroughly is demonstrated in (a) and (b), where the solvents used are methanol (MeOH) and dimethyl sulfoxide (DMSO) respectively. The change in characteristics of similar transistor channels after being submerged in these same solvents for one hour along with 1 mM PBASE then rinsed are shown in (c) and (d) respectively. Threshold voltages for each transfer characteristic are also shown.

channel conductance post-functionalisation for both Figure 1.4c and Figure 1.4d relative to the solvent-only case in Figure 1.4a and Figure 1.4b. It appears that the presence of PBASE molecules increases channel mobility and therefore conductance [47].

Capacitive gating results from dense coverage of adsorbed molecules on the carbon nanotube surface which have a low permittivity relative to the surrounding electrolyte [47]. The relative permittivity of MeOH and DMSO are ~ 33 [49] and ~ 47 [50] respectively, which are both much lower than the relative permittivity of phosphate buffer saline, ~ 80 [51]. From Figure 1.4a and Figure 1.4b, we find the average threshold shift values resulting from exposure to each solvent were $\Delta V = -0.15 \pm 0.03$ V and $\Delta V = -0.15 \pm 0.01$ for MeOH and DMSO respectively. The threshold voltage shifts in Figure 1.4c and Figure 1.4d from the pristine are small compared with the devices exposed to solvent only - this is likely due to the effect of increased conductance from the PBASE competing with the gating effect from the residual solvent.

This example illustrates why the use of electrical characteristics when making conclusions around a successful functionalisation process should individually take into account each substance used in the process. The qualitative presence of a change in characteristics (or lack of one) over the full process is not sufficient to make conclusive remarks about the electrical changes due to functionalisation. A full set of electrical control measurements are required for an understanding of electronic changes occuring during the functionalisation process, in the manner of Besteman *et al.* [16].

1.1.2. Other Pyrene-Based Linkers

Alongside PBASE, there are a wide range of other pyrene-based linker molecules used for modification of carbon nanotubes and graphene [52]. A few of these linkers are examined further below.

1-Pyrenebutyric Acid (PBA) with EDC/NHS

Another linker molecule that can be used to attach receptor molecules to a carbon nanotube or graphene channel is 1-pyrenebutyric acid (PBA). As with PBASE, the pyrene group of PBA has a π interaction with the carbon rings of the channel surface. It is possible to react PBA with 1-ethyl-3-(3-dimethylaminopropyl) carbodiimide hydrochloride (EDC or EDAC) to form an *O*-acylisourea intermediate, which can then react with an amine group on a biomolecule and form an amide bond [53], [54]. The water solubility of EDC means that, unlike PBASE, it is possible to functionalise with EDC dissolved in water rather than in an organic solvent. However, like PBASE, EDC and the *O*-acylisourea intermediate are prone to hydrolysis, especially in acidic conditions. Therefore, like

PBASE, it should be stored at $-20°$C, and warmed to room temperature to prevent condensation build-up, since exposure to condensation will hydrolyse the reagent [54]. Furthermore, by adding N-Hydroxysuccinimide (NHS) or N-hydroxysulfosuccinimide (sulfo-NHS) to the reaction vessel, PBASE is formed as an active intermediate, which is less prone to hydrolysis and increases the PBA/EDC reaction yield [53]–[55].

From Table 1.1 and Table 1.2, we see that PBASE is more widely used for non-covalent functionalisation than PBA/EDC. As was the case for PBASE, there are a wide range of process variables used for the functionalisation process, with little justification used for variables chosen. Also notable is the frequent use of polyethylene glycol (PEG) or pyrene-PEG for prevention of non-specific binding (see **?@sec-non-specific-binding** for further discussion of NSB). Despite being less widely useS, Mishyn *et al.* state a preference for the use of PBA/EDC over PBASE, as they found it was less prone to hydrolysis and gave a larger reaction yield when binding ferrocene to graphene [4]. A potential downside of using PBA/EDC for protein immobilisation is that EDC has numerous ways of interacting with proteins, and not all of these are necessarily desirable. The addition of NHS may also cause processing issues, such as precipitation of the reaction compound [54]. The greater range of process variables involved in the functionalisation also adds to the complexity of accurately reproducing past results.
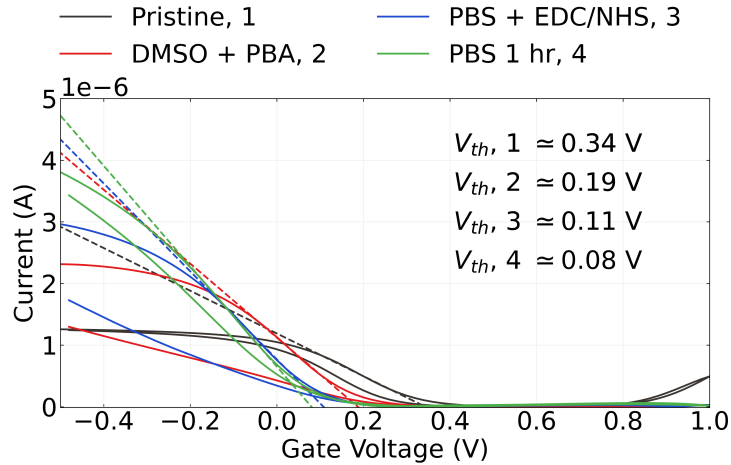

Figure 1.5.: Electrical transfer characteristics of a carbon nanotube transistor before functionalisation, after being submerged in DMSO containing 5 mM PBA for 1 hour, after being submerged in 1XPBS containing 20 mM EDC and 40 mM NHS for 30 min, then after being submerged in fresh 1XPBS for 1 hour. Threshold voltages for each transfer characteristic are also shown.

Table 1.2.: Comparison of 1-pyrenebutyric acid (PBA) functionalisation processes used for immobilisation of proteins and aptamers onto carbon nanotubes and graphene. 1-ethyl-3-(3-dimethylaminopropyl) carbodiimide hydrochloride (EDC) and NHS were co-mingled in buffer/electrolyte solution or DI water in each process - some papers used N-hydroxysulfosuccinimide instead of N-hydroxysuccinimide, and both compounds are abbreviated to NHS in this table. [†]PEG or PEG pyrene were used to reduce non-specific binding. [††]Several pyrene-based linkers were compared and PBA was found to give an optimal result.

Solvent	Channel	PBA (mM)	PBA Time (hr)	EDC (mM)	NHS (mM)	EDC/NHS Time (hr)	References
DMF	Graphene	0.6	1	-	-	120	Gao *et al.*[†] [56]
		5	2	2	5	30	Mishyn *et al.* [4]
	CNT	100	3	200	-	30	Min *et al.* [57]
DI water	CNT	-	-	32	12	Overnight	Pacios *et al.*[†] [58]
Ethanol	CNT	1	1	100	100	20	Filipiak *et al.*[†] [59]
Acetonitrile	Graphene	1	1	400	100	60	Tong *et al.*[††] [60]
Borax solution	CNT	2	24	2.5	-	1080	Liu *et al.*[†] [61]
DMSO	Graphene	5	1	50	50	90	Fenzl *et al.* [62]

Figure 1.5 shows the transfer characteristics of a carbon nanotube transistor at various stages of a PBA/EDC functionalisation, where a excess of N-hydroxysuccinimide (NHS) was added alongside EDC. The PBA was dissolved in DMSO, and the device channels were exposed to this solution for 1 hour. Subsequently, it was rinsed with 1XPBS and exposed to 20 mM EDC and 40 mM NHS in 1XPBS electrolyte for 30 minutes. We can compare Figure 1.5 to Figure 1.4 for a better understanding of the result of both the PBASE and PBA/EDC functionalisation methods. The threshold shift with the addition of 5 mM PBA in DMSO for 1 hour is equivalent to the shift seen when only DMSO is added, $\Delta V = -0.15$ V. The lack of a significant threshold shift is a result of pyrene having a neutral charge state, and any contributions from the charged carboxyl group being screened from the carbon nanotube sidewalls by surrounding water molecules [63]. However, as in the case of the addition of PBASE, there also appears to be an increase in hole mobility, which may be due to the pyrene groups increasing connectivity within the carbon nanotube network [48]. When EDC/NHS is added, a further increase in mobility of channel holes is seen [47].

Pyrene-NTA, Pyrene-Biotin and PEGylation

Through chemical coupling/conjugation, it is possible to replace the NHS ester group on PBASE with other groups that can undergo binding reactions with proteins. For example, PBASE can be modified with Nα,Nα-Bis(carboxymethyl)-L-lysine hydrate (also known as N-(5-Amino-1-carboxypentyl)iminodiacetic acid, AB-NTA) to produce pyrene-nitrilotriacetic acid (pyrene-NTA). The attached NTA group is able to chelate with metal ions such as Cu^{2+} or Ni^{2+}, which then can then coordinate with polyhistidine-tags attached to a protein [64], [65]. This functionalisation procedure was successfully used with mammalian odorant receptors attached via Ni^{2+} to a single carbon nanotube to detect eugenol vapour in real-time [66]. Pyrene-biotin (pyrene butanol biotin ester) can also be produced for attaching avidin or strepavidin [64]. As avidin and strepavidin are tetrameric, they can be attached to both pyrene-biotin and biotinylated proteins simultaneously via strong non-covalent bonding [67]–[70]. The use of protein his-tags and avi-tags for these binding processes means protein-transducer attachment can be better controlled than the amide bonding discussed earlier, with high specificity and directionality.

It is also possible to attach polyethylene glycol (PEG) chains to a pyrene group and modify them with reactive groups such as NTA and biotin to attach proteins in the same manner outlined in the previous paragraph [71], [72]. Once modified with PEG, pyrene linkers are also more water soluble, making it possible to perform a full functionalisation procedure exclusively in aqueous solution [71]. By setting the length of the PEG chain, the size of the linker molecule can be controlled - selection of a short chain is important for ensuring attached receptors remain within the Debye length of the transducer [73].

1.2. Verifying Pyrene Attachment to CNT network and Graphene

1.2.1. Photoresist contamination

1.2.2. Raman Spectroscopy

1.2.3. Pyrene-PEG-FITC fluorescence microscopy

Plasma clean comparison

Surfactant comparison

1.2.4. Pyrene-PEG electrical characterisation

A. Python Code for Data Analysis

A.1. Code Repository

The code used for general analysis of field-effect transistor devices in this thesis was written with Python 3.8.8. Contributors to the code used include Erica Cassie, Erica Happe, Marissa Dierkes and Leo Browning. The code is located on GitHub and the research group OneDrive, and is available on request.

A.2. Atomic Force Microscope Histogram Analysis

The purpose of this code is to analyse atomic force microscope (AFM) images of carbon nanotube networks in .xyz format taken using an atomic force microscope and processed in Gwyddion (see **?@sec-afm-characterisation**). It was originally designed by Erica Happe in Matlab, and adapted by Marissa Dierkes and myself for use in Python.

$$f(x) = k_1 \exp\left(-\frac{(x-m_1)^2}{2s_1{}^2}\right) + k_2 \exp\left(-\frac{(x-m_2)^2}{2s_2{}^2}\right) + ... \tag{A.1}$$

The .xyz data is initially sorted into bins with 0.15 nm size. The bin with the maximum number of counts is set at 0 nm, as this peak represents the mean of the surface roughness of the bare silicon. The parameters m_i, s_i, k_i (i = 1, 2, 3) are used with objective function Equation A.1 to overlay the data with normal distributions. These fitting parameters represent the mean (m), standard deviation (s) and amplitude (k) of each normal distribution. We can make approximations of some of these fitting parameters using the histogram data.

k_1 is taken to be the maximum y-value of the data being fitted, m_1 is set to zero (used as a point of reference) and s_1 is taken as one-third of the difference between m_1 and the x-value of the first datapoint where the y-value is greater than 1% of k_1 (approximating one standard deviation). We find the distribution given by these values using Equation A.1, and subtract it from the existing dataset.

Then, using the analysis technique outlined by Vobornik *et al.* [74] in Gwyddion, we manually find estimates for the mean m_2 and standard deviation s_2 of the carbon nanotube bundle distribution. We then take k_2 to be the maximum y-value of this modified

dataset, and m_1 to be the x-value of the maximum y-value. We then set k_2 so that the height of the resulting distribution at one standard deviation matches the height of the .xyz data histogram. We take this distribution, and subtract it from the existing dataset.

The code also allows for discretely binning continuous data from fitted normal distributions and examining the proportion of counts above or below a particular height. 2.9 nm is roughly where 2 bundles with average size 1.45 nm can start to be present, and is used as an estimate of the boundary value between single-tube bundle diameters and multi-tube bundle diameters.

A.3. Field-Effect Transistor Analysis

The purpose of this code is to analyse electrical measurements taken of field-effect transistor (FET) devices. Electrical measurements were either taken from the Keysight 4156C Semiconductor Parameter Analyser, National Instruments NI-PXIe or Keysight B1500A Semiconductor Device Analyser as discussed in **?@sec-electrical-characterisation**; the code is able to analyse data taken from all three measurement setups. The main Python file in the code base consists of three related but independent modules: the first analyses and plots sensing data from the FET devices, the second analyses and plots transfer characteristics from channels across a device, and the third compares individual channel characteristics before and after a modification or after each of several modifications. The code base also features a separate config file and style sheet which govern the behaviour of the main code. The code base was designed collaboratively by myself and Erica Cassie over GitHub using the Sourcetree Git GUI.

The first of the three modules is for processing sensing datasets. This module imports sensing measurements in .csv format and analyses them, then outputs a plot of the raw data, alongside multiple plots which have been modified in various ways. It can also fit exponential and linear trendlines to regions of the sensing data, as well as find the signal change per analyte addition, and returns spreadsheets containing the results of these analyses. These spreadsheets include the standard deviation for all included parameters. Modified plots include normalised plots (type of normalisation can be set in config file), plots with fitted curves, plots with the linear baseline drift removed, plots of signal with analyte addition, "despiked" plots and "filtered" plots. It is possible to add annotations to any of these plots using the config file, and it is possible to produce a plot with a combination of these modifications.

The scipy.optimize.curve_fit module is used to fit linear and exponential curves to regions of interest of the sensing data. Initial parameters for the scipy.optimize.curve_fit module are chosen by approximating fitting parameters in a similar manner to the approach in Section A.2. For a linear fit $mt + b$, the parameters are simply set as $m = 1$ and $b = 0$. For an exponential fit $a \exp(-t/\tau) + c$, c is set as the final current measurement of the

region of interest and a is set as the initial current measurement minus c. Then, τ is set as the time where current has dropped to $e^{-1}a + c$.

"Despiked" plots have had spurious datapoints removed through the use of an interquartile range rolling filter. The window size of the rolling filter used was 40 datapoints, and datapoints in each window with a z-score above ± 3 were removed from the plotted/processed data. "Filtered" plots had noise reduced using a moving median filter. The moving median filter is more effective at removing noise than a simple moving average, and has advantages over other filters (such as the Savitzky-Golay filter) when removing noise from data with sharp edges, as is the case for sensing data. Median filtering can also be used for baseline drift compensation, though this approach was not used in this thesis [75]. The moving median filter used had a window of 40 datapoints.

Plots of signal with analyte addition were constructed from current data after first removing baseline drift and applying a moving median filter. A simple difference calculation between the mean of the filtered current before an addition and the mean of the filtered current after the addition was performed at each addition. These differences were then normalised relative to the initial current. The signal with analyte addition give reasonably consistent results regardless of whether baseline drift was removed from the data, as shown in Figure A.1. We can therefore be confident that robust signal with analyte addition plots are robust even in the presence of significant drift.
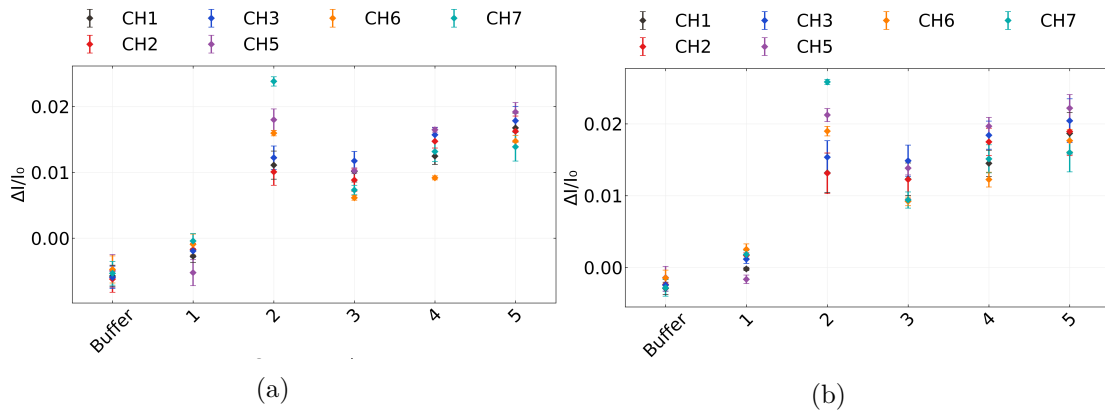

(a)

(b)

Figure A.1.: A comparison of signal with analyte addition plots taken from the same salt concentration sensing dataset (the same dataset as used in **?@fig-salt-conc-sensing**). In (a), a simple difference calculation performed on filtered data was used, while in (b) the same calculation was performed on filtered data with the baseline drift removed, the method used in the body of the thesis.

The second module imports transfer measurements in .csv format and creates combined and individual plots of the eight channels on a single device. In combined plots, channels which are non-working, due to being shorted or non-conducting, are removed via setting a maximum and minimum possible on-current in the config file. Various parameters from

the transfer characteristics are saved as a spreadsheet along with standard error. These parameters include on current, off current, subthreshold slope and threshold voltage for the carbon nanotube devices, and on current, off current and major Dirac point voltage for graphene devices. The device type being analysed can be set in the config file.

The third module imports several transfer measurements in .csv format and allows for comparison of the same channel before and after some modification. It also calculates the shift in either threshold voltage or major Dirac voltage of the device.

B. Vapour Delivery System

B.1. Technical Notes

Two LabView Virtual Instruments (VIs) were adapted from pre-existing VIs for operating the mass flow controllers and monitoring vapour flow into the device chamber, as well as monitoring temperature and humidity in the vapour delivery system's manifold. These VIs were named " " A third VI was developed in parallel which combined the first two Virtual Instruments, alongside allowing the sequence of values to control the mass flow controllers.

From Honours report: " " " Figure 12 gives the right side of the front panel of the LabView VI sample with vapour.VI, which letsus preset an autonomously-performed vapour sensing sequence. Each row in each array module corresponds to a differennest step in this sequence. The 'howManySteps' module lets us set how many of these steps are performed. The 'Durations Array' module determines the length of time in seconds each step is performed over. The 'Carrier Flows Array' and 'Dilution Flows Array' modules let us set the carrier flow and dilution flow, respectively, in standard cubic centimetres per minute (sccm) through the gas rig at each step. The carrier flow pushes analyte vapour into the vapour-sensing device chamber, while dilution flow is used to modify the flow behaviour of the analyte vapour entering the chamber. The vapour sensing sequence as depicted in Figure 12 was used for all vapour sensing runs in this investigation. At the end of the sequence, the data collected about the vapour sensing process was saved as an .lvm file. " " "

B.2. Future Improvements

Bibliography

[1] Brenda Long, Mary Manning, Micheal Burke, et al. "Non-Covalent Functionalization of Graphene Using Self-Assembly of Alkane-Amines". In: *Advanced Functional Materials* 22.4 (Feb. 2012), pp. 717–725. ISSN: 1616-3028. DOI: 10.1002/ADFM.201101956. URL: https://onlinelibrary.wiley.com/doi/full/10.1002/adfm.201101956%20https://onlinelibrary.wiley.com/doi/abs/10.1002/adfm.201101956%20https://onlinelibrary.wiley.com/doi/10.1002/adfm.201101956.

[2] Antonello Di Crescenzo, Valeria Ettorre, and Antonella Fontana. "Non-covalent and reversible functionalization of carbon nanotubes". In: *Beilstein Journal of Nanotechnology* 5.1 (2014), p. 1675. ISSN: 21904286. DOI: 10.3762/BJNANO.5.178. URL: /pmc/articles/PMC4222398/%20/pmc/articles/PMC4222398/?report=abstract%20https://www.ncbi.nlm.nih.gov/pmc/articles/PMC4222398/.

[3] Shiyu Wang, Md Zakir Hossain, Kazuo Shinozuka, et al. "Graphene field-effect transistor biosensor for detection of biotin with ultrahigh sensitivity and specificity". In: *Biosensors and Bioelectronics* 165 (Oct. 2020), p. 112363. ISSN: 18734235. DOI: 10.1016/J.BIOS.2020.112363. URL: /pmc/articles/PMC7272179/%20/pmc/articles/PMC7272179/?report=abstract%20https://www.ncbi.nlm.nih.gov/pmc/articles/PMC7272179/.

[4] Vladyslav Mishyn, Adrien Hugo, Teresa Rodrigues, et al. "The holy grail of pyrene-based surface ligands on the sensitivity of graphene-based field effect transistors". In: *Sensors and Diagnostics* 1.2 (Mar. 2022), pp. 235–244. ISSN: 2635-0998. DOI: 10.1039/D1SD00036E. URL: https://pubs.rsc.org/en/content/articlehtml/2022/sd/d1sd00036e%20https://pubs.rsc.org/en/content/articlelanding/2022/sd/d1sd00036e.

[5] Mitchell B. Lerner, Felipe Matsunaga, Gang Hee Han, et al. "Scalable production of highly sensitive nanosensors based on graphene functionalized with a designed G protein-coupled receptor". In: *Nano Letters* 14.5 (May 2014), pp. 2709–2714. ISSN: 15306992. DOI: 10.1021/NL5006349/SUPPL_FILE/NL5006349_SI_001.PDF. URL: https://pubs.acs.org/doi/full/10.1021/nl5006349.

[6] Kishan Thodkar, Pierre Andre Cazade, Frank Bergmann, et al. "Self-assembled pyrene stacks and peptide monolayers tune the electronic properties of functionalized electrolyte-gated graphene field-effect transistors". In: *ACS Applied Materials and Interfaces* 13.7 (Feb. 2021), pp. 9134–9142. ISSN: 19448252. DOI: 10.1021/ACSAMI.0C18485/ASSET/IMAGES/LARGE/AM0C18485_0006.JPEG. URL: https://pubs.acs.org/doi/full/10.1021/acsami.0c18485.

[7]   Emilio M. Pérez and Nazario Martín. "π–π interactions in carbon nanostructures". In: *Chemical Society Reviews* 44.18 (Sept. 2015), pp. 6425–6433. ISSN: 1460-4744. DOI: 10.1039/C5CS00578G. URL: https://pubs.rsc.org/en/content/articlehtml /2015/cs/c5cs00578g%20https://pubs.rsc.org/en/content/articlelanding/2015/cs /c5cs00578g.

[8]   Chelsea R. Martinez and Brent L. Iverson. "Rethinking the term "pi-stacking"". In: *Chemical Science* 3.7 (June 2012), pp. 2191–2201. ISSN: 2041-6539. DOI: 10.10 39/C2SC20045G. URL: https://pubs.rsc.org/en/content/articlehtml/2012/sc/c2s c20045g%20https://pubs.rsc.org/en/content/articlelanding/2012/sc/c2sc20045g.

[9]   Greg T. Hermanson. "Buckyballs, Fullerenes, and Carbon Nanotubes". In: *Bioconjugate Techniques* (Jan. 2013), pp. 741–755. DOI: 10.1016/B978-0-12-382239-0.00 016-9.

[10] Carbonnanotube. *File:Noncovalent carboncarbonnanotube.png.* 2015. URL: https: //en.m.wikipedia.org/wiki/File:Noncovalent_carboncarbonnanotube.png (visited on 2023-10-13).

[11] Kenzo Maehashi, Taiji Katsura, Kagan Kerman, et al. "Label-free protein biosensor based on aptamer-modified carbon nanotube field-effect transistors". In: *Analytical Chemistry* 79.2 (Jan. 2007), pp. 782–787. ISSN: 00032700. DOI: 10.1021/ac060830g. URL: https://pubs.acs.org/doi/full/10.1021/ac060830g.

[12] Cristina García-Aljaro, Lakshmi N. Cella, Dhamanand J. Shirale, et al. "Carbon nanotubes-based chemiresistive biosensors for detection of microorganisms". In: *Biosensors and Bioelectronics* 26.4 (Dec. 2010), pp. 1437–1441. ISSN: 09565663. DOI: 10.1016/j.bios.2010.07.077.

[13] R. J. Chen, Y. Zhang, D. Wang, et al. "Noncovalent sidewall functionalization of single-walled carbon nanotubes for protein immobilization". In: *Journal of the American Chemical Society* 123.16 (2001), pp. 3838–3839. ISSN: 00027863. DOI: 10.1021/ja010172b. URL: http://pubs.acs.org..

[14] Lakshmi N. Cella, Pablo Sanchez, Wenwan Zhong, et al. "Nano aptasensor for Protective Antigen Toxin of Anthrax". In: *Analytical Chemistry* 82.5 (Mar. 2010), pp. 2042–2047. ISSN: 00032700. DOI: 10.1021/ac902791q. URL: https://pubs.acs .org/doi/full/10.1021/ac902791q.

[15] Basanta K. Das, Chaker Tlili, Sushmee Badhulika, et al. "Single-walled carbon nanotubes chemiresistor aptasensors for small molecules: Picomolar level detection of adenosine triphosphate". In: *Chemical Communications* 47.13 (Mar. 2011), pp. 3793–3795. ISSN: 1364548X. DOI: 10.1039/c0cc04733c. URL: https://pubs.rs c.org/en/content/articlehtml/2011/cc/c0cc04733c%20https://pubs.rsc.org/en/co ntent/articlelanding/2011/cc/c0cc04733c.

[16] Koen Besteman, Jeong O. Lee, Frank G.M. Wiertz, et al. "Enzyme-coated carbon nanotubes as single-molecule biosensors". In: *Nano Letters* 3.6 (June 2003), pp. 727– 730. ISSN: 15306984. DOI: 10.1021/NL034139U/ASSET/IMAGES/LARGE/NL0 34139UF00004.JPEG. URL: https://pubs.acs.org/doi/full/10.1021/nl034139u.

[17]   Deana Kwong Hong Tsang, Tyler J. Lieberthal, Clare Watts, et al. "Chemically Functionalised Graphene FET Biosensor for the Label-free Sensing of Exosomes". In: *Scientific Reports* 9.1 (Sept. 2019), pp. 1–10. ISSN: 20452322. DOI: 10.1038/s 41598-019-50412-9. URL: https://www.nature.com/articles/s41598-019-50412-9.

[18]   Gregory R. Wiedman, Yanan Zhao, Arkady Mustaev, et al. "An Aptamer-Based Biosensor for the Azole Class of Antifungal Drugs". In: *mSphere* 2.4 (Aug. 2017). ISSN: 23795042. DOI: 10.1128/msphere.00274-17. URL: /pmc/articles/PMC5566 834/%20/pmc/articles/PMC5566834/?report=abstract%20https://www.ncbi.nl m.nih.gov/pmc/articles/PMC5566834/.

[19]   Zhaoli Gao, Han Xia, Jonathan Zauberman, et al. "Detection of Sub-fM DNA with Target Recycling and Self-Assembly Amplification on Graphene Field-Effect Biosensors". In: *Nano Letters* 18.6 (June 2018), pp. 3509–3515. ISSN: 15306992. DOI: 10.1021/acs.nanolett.8b00572. URL: https://pubs.acs.org/doi/full/10.1021 /acs.nanolett.8b00572.

[20]   Nikita Nekrasov, Natalya Yakunina, Averyan V. Pushkarev, et al. "Spectral-phase interferometry detection of ochratoxin a via aptamer-functionalized graphene coated glass". In: *Nanomaterials* 11.1 (Jan. 2021), pp. 1–10. ISSN: 20794991. DOI: 10.3390/nano11010226. URL: https://www.mdpi.com/2079-4991/11/1/226/htm %20https://www.mdpi.com/2079-4991/11/1/226.

[21]   Michael T. Hwang, B. Landon Preston, Lee Joon, et al. "Highly specific SNP detection using 2D graphene electronics and DNA strand displacement". In: *Proceedings of the National Academy of Sciences of the United States of America* 113.26 (June 2016), pp. 7088–7093. ISSN: 10916490. DOI: 10.1073/pnas.1603753113. URL: https://www.pnas.org/doi/abs/10.1073/pnas.1603753113.

[22]   Zhuang Hao, Yunlu Pan, Cong Huang, et al. "Modulating the Linker Immobilization Density on Aptameric Graphene Field Effect Transistors Using an Electric Field". In: *ACS Sensors* 5.8 (Aug. 2020), pp. 2503–2513. ISSN: 23793694. DOI: 10.1021/ACSSENSORS.0C00752/ASSET/IMAGES/LARGE/SE0C00752_0008 .JPEG. URL: https://pubs.acs.org/doi/full/10.1021/acssensors.0c00752.

[23]   Mohd Maidin Nur Nasyifa, A. Rahim Ruslinda, Nur Hamidah Abdul Halim, et al. "Immuno-probed graphene nanoplatelets on electrolyte-gated field-effect transistor for stable cortisol quantification in serum". In: *Journal of the Taiwan Institute of Chemical Engineers* 117 (Dec. 2020), pp. 10–18. ISSN: 18761070. DOI: 10.1016/j.j tice.2020.12.008.

[24]   Rui Campos, Jérôme Borme, Joana Rafaela Guerreiro, et al. "Attomolar label-free detection of dna hybridization with electrolyte-gated graphene field-effect transistors". In: *ACS Sensors* 4.2 (Feb. 2019), pp. 286–293. ISSN: 23793694. DOI: 10.10 21/acssensors.8b00344. URL: https://pubs.acs.org/doi/full/10.1021/acssensors.8 b00344.

[25] Murat Kuscu, Hamideh Ramezani, Ergin Dinc, et al. "Graphene-based Nanoscale Molecular Communication Receiver: Fabrication and Microfluidic Analysis". In: (June 2020). arXiv: 2006.15470. URL: https://arxiv.org/abs/2006.15470v2.

[26] Shicai Xu, Jian Zhan, Baoyuan Man, et al. "Real-time reliable determination of binding kinetics of DNA hybridization using a multi-channel graphene biosensor". In: *Nature Communications* 8.1 (Mar. 2017), pp. 1–10. ISSN: 20411723. DOI: 10 .1038/ncomms14902. URL: https://www.nature.com/articles/ncomms14902.

[27] Niazul I. Khan, Mohammad Mousazadehkasin, Sujoy Ghosh, et al. "An integrated microfluidic platform for selective and real-time detection of thrombin biomarkers using a graphene FET". In: *Analyst* 145.13 (June 2020), pp. 4494–4503. ISSN: 13645528. DOI: 10.1039/d0an00251h. URL: https://pubs.rsc.org/en/content/arti clehtml/2020/an/d0an00251h%20https://pubs.rsc.org/en/content/articlelanding /2020/an/d0an00251h.

[28] T Ono, K Kamada, R Hayashi, et al. "Lab-on-a-graphene-FET detection of key molecular events underpinning influenza 2 virus infection and effect of antiviral drugs 3 Running title: Graphene-FET detects reactions in an influenza infection MAIN TEXT". In: *bioRxiv* (Mar. 2020), p. 2020.03.18.996884. DOI: 10.1101/2020 .03.18.996884. URL: https://doi.org/10.1101/2020.03.18.996884.

[29] Han Yue Zheng, Omar A. Alsager, Bicheng Zhu, et al. "Electrostatic gating in carbon nanotube aptasensors". In: *Nanoscale* 8.28 (July 2016), pp. 13659–13668. ISSN: 20403372. DOI: 10.1039/c5nr08117c. URL: https://pubs.rsc.org/en/conten t/articlehtml/2016/nr/c5nr08117c%20https://pubs.rsc.org/en/content/articlelan ding/2016/nr/c5nr08117c.

[30] Jun Pyo Kim, Byung Yang Lee, Joohyung Lee, et al. "Enhancement of sensitivity and specificity by surface modification of carbon nanotubes in diagnosis of prostate cancer based on carbon nanotube field effect transistors". In: *Biosensors and Bio-electronics* 24.11 (July 2009), pp. 3372–3378. ISSN: 09565663. DOI: 10.1016/j.bio s.2009.04.048. URL: https://pubmed.ncbi.nlm.nih.gov/19481922/.

[31] Jin Yoo, Daesan Kim, Heehong Yang, et al. "Olfactory receptor-based CNT-FET sensor for the detection of DMMP as a simulant of sarin". In: *Sensors and Actuators B: Chemical* 354 (Mar. 2022), p. 131188. ISSN: 0925-4005. DOI: 10.1016/J.SNB.2 021.131188.

[32] Jagriti Sethi, Michiel Van Bulck, Ahmed Suhail, et al. "A label-free biosensor based on graphene and reduced graphene oxide dual-layer for electrochemical determination of beta-amyloid biomarkers". In: *Microchimica Acta* 187.5 (May 2020), pp. 1– 10. ISSN: 14365073. DOI: 10.1007/s00604-020-04267-x. URL: https://link.spring er.com/article/10.1007/s00604-020-04267-x.

[33] Yasuhide Ohno, Kenzo Maehashi, and Kazuhiko Matsumoto. "Label-free biosensors based on aptamer-modified graphene field-effect transistors". In: *Journal of the American Chemical Society* 132.51 (Dec. 2010), pp. 18012–18013. ISSN: 00027863. DOI: 10.1021/ja108127r. URL: https://pubs.acs.org/doi/full/10.1021/ja108127r.

[34] Ryan J. Lopez, Sofia Babanova, Kateryna Artyushkova, et al. "Surface modifi-
cations for enhanced enzyme immobilization and improved electron transfer of
PQQ-dependent glucose dehydrogenase anodes". In: *Bioelectrochemistry* 105 (Oct.
2015), pp. 78–87. ISSN: 1878562X. DOI: 10.1016/j.bioelechem.2015.05.010. URL:
https://pubmed.ncbi.nlm.nih.gov/26011132/.

[35] Guinevere Strack, Robert Nichols, Plamen Atanassov, et al. "Modification of car-
bon nanotube electrodes with 1-pyrenebutanoic acid, succinimidyl ester for en-
hanced bioelectrocatalysis". In: *Methods in Molecular Biology* 1051 (2013), pp. 217–
228. ISSN: 10643745. DOI: 10.1007/978-1-62703-550-7_14. URL: https://pubme
d.ncbi.nlm.nih.gov/23934807/.

[36] J. A. M. J. Frisch and G. W. Trucks and H. B. Schlegel and G. E. Scuseria and
M. A. Robb and J. R. Cheeseman and G. Scalmani and V. Barone and G. A.
Petersson and H. Nakatsuji and X. Li and M. Caricato and A. V. Marenich and J.
Bloino and B. G. Janesko and R. G, J. E. Peralta, F. Ogliaro, et al. *Gaussian˜16
Revision C.01*. 2016.

[37] Yasuhiro Oishi, Hirotsugu Ogi, Satoshi Hagiwara, et al. "Theoretical Analysis on
the Stability of 1-Pyrenebutanoic Acid Succinimidyl Ester Adsorbed on Graphene".
In: *ACS Omega* 7.35 (Sept. 2022), pp. 31120–31125. ISSN: 24701343. DOI: 10.10
21/ACSOMEGA.2C03257/ASSET/IMAGES/LARGE/AO2C03257_0004.JPEG.
URL: https://pubs.acs.org/doi/full/10.1021/acsomega.2c03257.

[38] Greg T. Hermanson. "The Reactions of Bioconjugation". In: *Bioconjugate Tech-
niques* (Jan. 2013), pp. 229–258. DOI: 10.1016/B978-0-12-382239-0.00003-0.

[39] Malkolm Hinnemo, Jie Zhao, Patrik Ahlberg, et al. "On Monolayer Formation of
Pyrenebutyric Acid on Graphene". In: *Langmuir* 33.15 (Apr. 2017), pp. 3588–3593.
ISSN: 15205827. DOI: 10.1021/ACS.LANGMUIR.6B04237/ASSET/IMAGES/L
ARGE/LA-2016-04237V_0003.JPEG. URL: https://pubs.acs.org/doi/full/10.10
21/acs.langmuir.6b04237.

[40] Xue V. Zhen, Emily G. Swanson, Justin T. Nelson, et al. "Noncovalent monolayer
modification of graphene using pyrene and cyclodextrin receptors for chemical
sensing". In: *ACS Applied Nano Materials* 1.6 (June 2018), pp. 2718–2726. ISSN:
25740970. DOI: 10.1021/ACSANM.8B00420/ASSET/IMAGES/LARGE/AN-201
8-00420J_0004.JPEG. URL: https://pubs.acs.org/doi/full/10.1021/acsanm.8b00
420.

[41] Ryan J. White, Noelle Phares, Arica A. Lubin, et al. "Optimization of electro-
chemical aptamer-based sensors via optimization of probe packing density and
surface chemistry". In: *Langmuir : the ACS journal of surfaces and colloids* 24.18
(Sept. 2008), pp. 10513–10518. ISSN: 0743-7463. DOI: 10.1021/LA800801V. URL:
https://pubmed.ncbi.nlm.nih.gov/18690727/.

[42] Yu Chen, Tze Sian Pui, Patthara Kongsuphol, et al. "Aptamer-based array electrodes for quantitative interferon-γ detection". In: *Biosensors and Bioelectronics* 53 (Mar. 2014), pp. 257–262. ISSN: 1873-4235. DOI: 10.1016/J.BIOS.2013.09.046. URL: https://pubmed.ncbi.nlm.nih.gov/24144556/.

[43] Greg T. Hermanson. "Homobifunctional Crosslinkers". In: *Bioconjugate Techniques* (Jan. 2013), pp. 275–298. DOI: 10.1016/B978-0-12-382239-0.00005-4.

[44] *1-Pyrenebutyric acid N-hydroxysuccinimide ester - [1H NMR] - Spectrum - SpectraBase*. URL: https://spectrabase.com/spectrum/FxRoJanrm9t (visited on 2023-10-19).

[45] R. G. Lebel and D. A.I. Goring. "Density, Viscosity, Refractive Index, and Hygroscopicity of Mixtures of Water and Dimethyl Sulfoxide". In: *Journal of Chemical and Engineering Data* 7.1 (Jan. 1962), pp. 100–101. ISSN: 15205134. DOI: 10.1021/JE60012A032/ASSET/JE60012A032.FP.PNG_V03. URL: https://pubs.acs.org/doi/abs/10.1021/je60012a032.

[46] Alexander B. Artyukhin, Michael Stadermann, Raymond W. Friddle, et al. "Controlled electrostatic gating of carbon nanotube FET devices". In: *Nano Letters* 6.9 (Sept. 2006), pp. 2080–2085. ISSN: 15306984. DOI: 10.1021/NL061343J/SUPPL_FILE/NL061343JSI20060609_104449.PDF. URL: https://pubs.acs.org/doi/full/10.1021/nl061343j.

[47] Iddo Heller, Anne M. Janssens, Jaan Männik, et al. "Identifying the mechanism of biosensing with carbon nanotube transistors". In: *Nano Letters* 8.2 (Feb. 2008), pp. 591–595. ISSN: 15306984. DOI: 10.1021/NL072996I/SUPPL_FILE/NL072996ISI20071116_124235.PDF. URL: https://pubs.acs.org/doi/full/10.1021/nl072996i.

[48] Thanihaichelvan Murugathas, Han Yue Zheng, Damon Colbert, et al. "Biosensing with Insect Odorant Receptor Nanodiscs and Carbon Nanotube Field-Effect Transistors". In: *ACS Applied Materials and Interfaces* 11.9 (Mar. 2019), pp. 9530–9538. ISSN: 19448252. DOI: 10.1021/ACSAMI.8B19433/ASSET/IMAGES/LARGE/AM-2018-19433U_0002.JPEG. URL: https://pubs.acs.org/doi/full/10.1021/acsami.8b19433.

[49] M. Mohsen-Nia, H. Amiri, and B. Jazi. "Dielectric constants of water, methanol, ethanol, butanol and acetone: Measurement and computational study". In: *Journal of Solution Chemistry* 39.5 (2010), pp. 701–708. ISSN: 00959782. DOI: 10.1007/S10953-010-9538-5.

[50] Johannes Hunger, Richard Buchner, Mohamed E. Kandil, et al. "Relative permittivity of dimethylsulfoxide and N, N -dimethylformamide at temperatures from (278 to 328) K and pressures from (0.1 to 5) MPa". In: *Journal of Chemical and Engineering Data* 55.5 (May 2010), pp. 2055–2065. ISSN: 00219568. DOI: 10.1021/JE9010773/SUPPL_FILE/JE9010773_SI_001.PDF. URL: https://pubs.acs.org/doi/full/10.1021/je9010773.

[51] Alireza Salmanzadeh, Michael B. Sano, Roberto C. Gallo-Villanueva, et al. "Investigating dielectric properties of different stages of syngeneic murine ovarian cancer cells". In: *Biomicrofluidics* 7.1 (Feb. 2013). ISSN: 19321058. DOI: 10.1063/1.4788 921. URL: /pmc/articles/PMC3568086/%20/pmc/articles/PMC3568086/?report =abstract%20https://www.ncbi.nlm.nih.gov/pmc/articles/PMC3568086/.

[52] Yan Zhou, Yi Fang, and Ramaraja P. Ramasamy. "Non-Covalent Functionalization of Carbon Nanotubes for Electrochemical Biosensor Development". In: *Sensors (Basel, Switzerland)* 19.2 (Jan. 2019). ISSN: 1424-8220. DOI: 10.3390/S19020392. URL: https://pubmed.ncbi.nlm.nih.gov/30669367/.

[53] Deepak Sehgal and Inder K. Vijay. "A Method for the High Efficiency of Water-Soluble Carbodiimide-Mediated Amidation". In: *Analytical Biochemistry* 218.1 (Apr. 1994), pp. 87–91. ISSN: 0003-2697. DOI: 10.1006/ABIO.1994.1144.

[54] Greg T. Hermanson. "Zero-Length Crosslinkers". In: *Bioconjugate Techniques* (Jan. 2013), pp. 259–273. DOI: 10.1016/B978-0-12-382239-0.00004-2.

[55] Greg T. Hermanson. "Microparticles and Nanoparticles". In: *Bioconjugate Techniques* (Jan. 2013), pp. 549–587. DOI: 10.1016/B978-0-12-382239-0.00014-5.

[56] Ning Gao, Teng Gao, Xiao Yang, et al. "Specific detection of biomolecules in physiological solutions using graphene transistor biosensors". In: *Proceedings of the National Academy of Sciences of the United States of America* 113.51 (Dec. 2016), pp. 14633–14638. ISSN: 10916490. DOI: 10.1073/PNAS.1625010114/SUPP L_FILE/PNAS.201625010SI.PDF. URL: https://www.pnas.org/doi/abs/10.1073 /pnas.1625010114.

[57] Kyoungseon Min, Jungbae Kim, Kyungmoon Park, et al. "Enzyme immobilization on carbon nanomaterials: Loading density investigation and zeta potential analysis". In: *Journal of Molecular Catalysis B: Enzymatic* 83 (Nov. 2012), pp. 87–93. ISSN: 1381-1177. DOI: 10.1016/J.MOLCATB.2012.07.009.

[58] Mercè Pacios, Iñigo Martin-Fernandez, Xavier Borrisé, et al. "Real time protein recognition in a liquid-gated carbon nanotube field-effect transistor modified with aptamers". In: *Nanoscale* 4.19 (Sept. 2012), pp. 5917–5923. ISSN: 2040-3372. DOI: 10.1039/C2NR31257C. URL: https://pubs.rsc.org/en/content/articlehtml/2012 /nr/c2nr31257c%20https://pubs.rsc.org/en/content/articlelanding/2012/nr/c2nr 31257c.

[59] Marcin S. Filipiak, Marcel Rother, Nesha M. Andoy, et al. "Highly sensitive, selective and label-free protein detection in physiological solutions using carbon nanotube transistors with nanobody receptors". In: *Sensors and Actuators B: Chemical* 255 (Feb. 2018), pp. 1507–1516. ISSN: 0925-4005. DOI: 10.1016/J.SNB.2017.08.1 64.

[60] Jing Tong, Lei Zhang, Yi Wang, et al. "High response photodetection by applying the optimized photoreceptor protein modification on graphene based field effect transistors". In: *FrMat* 7 (July 2020), p. 222. ISSN: 22968016. DOI: 10.3389/FMA TS.2020.00222. URL: https://ui.adsabs.harvard.edu/abs/2020FrMat...7..222T/a bstract.

[61] Jie Liu, Florence Appaix, Olivier Bibari, et al. "Control of neuronal network organization by chemical surface functionalization of multi-walled carbon nanotube arrays". In: *Nanotechnology* 22.19 (May 2011). ISSN: 1361-6528. DOI: 10.1088/09 57-4484/22/19/195101. URL: https://pubmed.ncbi.nlm.nih.gov/21436508/.

[62] Christoph Fenzl, Pranati Nayak, Thomas Hirsch, et al. "Laser-Scribed Graphene Electrodes for Aptamer-Based Biosensing". In: *ACS sensors* 2.5 (May 2017), pp. 616–620. ISSN: 2379-3694. DOI: 10.1021/ACSSENSORS.7B00066. URL: https://pubmed.ncbi.nlm.nih.gov/28723173/.

[63] Mitchell B. Lerner, James M. Resczenski, Akshay Amin, et al. "Toward quantifying the electrostatic transduction mechanism in carbon nanotube molecular sensors". In: *Journal of the American Chemical Society* 134.35 (Sept. 2012), pp. 14318–14321. ISSN: 00027863. DOI: 10.1021/JA306363V/SUPPL_FILE/JA306363V_SI_001 .PDF. URL: https://pubs.acs.org/doi/full/10.1021/ja306363v.

[64] Michael Holzinger, Jessica Baur, Raoudha Haddad, et al. "Multiple functionalization of single-walled carbon nanotubes by dip coating". In: *Chemical Communications* 47.8 (Feb. 2011), pp. 2450–2452. ISSN: 1364-548X. DOI: 10.1039/C0CC039 28D. URL: https://pubs.rsc.org/en/content/articlehtml/2011/cc/c0cc03928d%20 https://pubs.rsc.org/en/content/articlelanding/2011/cc/c0cc03928d.

[65] Yoshihisa Amano, Ayako Koto, Shohei Matsuzaki, et al. "Construction of a biointerface on a carbon nanotube surface for efficient electron transfer". In: *Materials Letters* 174 (July 2016), pp. 184–187. ISSN: 0167-577X. DOI: 10.1016/J.MATLE T.2016.03.113.

[66] Brett R. Goldsmith, Joseph J. Mitala, Jesusa Josue, et al. "Biomimetic chemical sensors using nanoelectronic readout of olfactory receptor proteins". In: *ACS Nano* 5.7 (July 2011), pp. 5408–5416. ISSN: 19360851. DOI: 10.1021/NN200489J/SUP PL_FILE/NN200489J_SI_001.PDF. URL: https://pubs.acs.org/doi/full/10.102 1/nn200489j.

[67] Alexander Star, Jean Christophe P. Gabriel, Keith Bradley, et al. "Electronic detection of specific protein binding using nanotube FET devices". In: *Nano Letters* 3.4 (Apr. 2003), pp. 459–463. ISSN: 15306984. DOI: 10.1021/NL0340172 /SUPPL_FILE/NL0340172SI20030213_114154.PDF. URL: https://pubs.acs.org /doi/full/10.1021/nl0340172.

[68] Christopher M. Dundas, Daniel Demonte, and Sheldon Park. "Streptavidin-biotin technology: Improvements and innovations in chemical and biological applications". In: *Applied Microbiology and Biotechnology* 97.21 (Nov. 2013), pp. 9343–9353. ISSN:

01757598. DOI: 10.1007/S00253-013-5232-Z/FIGURES/3. URL: https://link.spri
nger.com/article/10.1007/s00253-013-5232-z.

[69]   Greg T. Hermanson. "(Strept)avidin–Biotin Systems". In: *Bioconjugate Techniques*
(Jan. 2013), pp. 465–505. DOI: 10.1016/B978-0-12-382239-0.00011-X.

[70]   Michael Fairhead and Mark Howarth. "Site-specific biotinylation of purified pro-
teins using BirA". In: *Methods in molecular biology (Clifton, N.J.)* 1266 (2015),
p. 171. ISSN: 10643745. DOI: 10.1007/978-1-4939-2272-7_12. URL: /pmc/article
s/PMC4304673/%20/pmc/articles/PMC4304673/?report=abstract%20https://w
ww.ncbi.nlm.nih.gov/pmc/articles/PMC4304673/.

[71]   Greg T. Hermanson. "PEGylation and Synthetic Polymer Modification". In: *Bio-
conjugate Techniques* (Jan. 2013), pp. 787–838. DOI: 10.1016/B978-0-12-382239-
0.00018-2.

[72]   Mehdi Meran, Pelin Deniz Akkus, Ozge Kurkcuoglu, et al. "Noncovalent Pyrene-
Polyethylene Glycol Coatings of Carbon Nanotubes Achieve in Vitro Biocompat-
ibility". In: *Langmuir* 34.40 (Oct. 2018), pp. 12071–12082. ISSN: 15205827. DOI:
10.1021/ACS.LANGMUIR.8B00971. URL: https://pubs.acs.org/doi/full/10.1021
/acs.langmuir.8b00971.

[73]   Bajramshahe Shkodra, Mattia Petrelli, Martina Aurora Costa Angeli, et al.
"Electrolyte-gated carbon nanotube field-effect transistor-based biosensors: Prin-
ciples and applications". In: *Applied Physics Reviews* 8.4 (Dec. 2021), p. 41325.
ISSN: 19319401. DOI: 10.1063/5.0058591/1076095. URL: /aip/apr/article/8/4/0
41325/1076095/Electrolyte-gated-carbon-nanotube-field-effect.

[74]   Dusan Vobornik, Maohui Chen, Shan Zou, et al. "Measuring the Diameter of Single-
Wall Carbon Nanotubes Using AFM". In: *Nanomaterials* 13.3 (Feb. 2023), p. 477.
ISSN: 20794991. DOI: 10.3390/NANO13030477/S1. URL: https://www.mdpi.co
m/2079-4991/13/3/477/htm%20https://www.mdpi.com/2079-4991/13/3/477.

[75]   David C. Stone. "Application of median filtering to noisy data". In: 73.10 (Oct.
2011), pp. 1573–1581. ISSN: 0008-4042. DOI: 10.1139/V95-195. URL: https://cd
nsciencepub.com/doi/10.1139/v95-195.